Supplementary Information

On the mechanism of iron oxide-induced macrophage activation: the impact of composition and the underlying signaling pathway

Zhengying Gu[1], Tianqing Liu[2], Jie Tang[1], Yannan Yang[1], Hao Song[1], Zewen K. Tuong[3], Jianye Fu[1], Chengzhong Yu[1, 4]*

1. Australian Institute for Bioengineering and Nanotechnology, the University of Queensland, Brisbane, Queensland 4072, Australia

2. QIMR Berghofer Medical Research Institute, 300 Herston Road, Brisbane, QLD, 4006, Australia

3. The University of Queensland Diamantina Institute, Translational Research Institute, Woolloongabba, Queensland, Australia

4. School of Chemistry and Molecular Engineering, East China Normal University, Shanghai 200241, People's Republic of China

Experimental:

Chemicals

Iron (III) chloride ($FeCl_3$), sodium phosphate monobasic (NaH_2PO_4), triethanolamine (TEA), cetyltrimethylammonium bromide (CTAB), sodium salicylate (NaSal) and tetraethyl orthosilicate (TEOS) were all purchased from Sigma-Aldrich.

Synthesis of IONP@D-SiO_2 and D-SiO_2 nanoparticles

Ellipsoidal hematite IONPs were prepared, then used as the core to grow a large-pore dendritic silica shell according to literature methods with slight modifications.[1-2]

1) Ellipsoidal hematite IONPs: Briefly, 1.62 g of $FeCl_3$ and 0.012 g NaH_2PO_4 were added to 500 mL of deionized water (diH_2O). The clear yellow solution was under hydrothermal treatment in autoclave at 100°C for 2 days. Then, the ellipsoidal hematite IONPs were collected, followed by washing with water for three times. The products were then dried in air at 50°C for 12 h.

2) IONP@D-SiO_2 and D-SiO_2: 160 mg of hematite IONPs were well dispersed in solution containing 0.034 g of TEA, 0.19 g of CTAB, 0.063 g of NaSal and 12.5 mL of diH_2O. The solution was vigorously stirred at 80°C for 3 h. Then, 1.8 mL of TEOS was added to above solution, followed by stirring at 80°C for 45 min. The as-prepared particles were collected by centrifugation at 4000 rpm for 15 min. The particles were washed with ethanol and deionized water for several times. The product was dried in air at 50°C for 12 h. Then, Fe_2O_3@D-SiO_2 nanoparticles was calcined in air at 550°C for 5 h to remove residual surfactant in nanoparticles. Fe_3O_4@D-SiO_2 nanoparticles were obtained by annealing Fe_2O_3@D-SiO_2 in H_2/N_2 atmosphere under 450°C for 3h with a ramping rate of 3°C/min. To obtain D-SiO_2 nanoparticles, Fe_3O_4@D-SiO_2 was suspended in 2M HCl/ethanol solution and stirred at 60°C for 12 h. Finally, D-SiO_2 was collected, washed and dried.

Characterizations:

The morphology of IONPs, IONP@D-SiO_2 and D-SiO_2 was characterized by transmission electron microscopy (TEM) using a JEOL 7700 microscope operated at 100 kV and scanning electron microscopy (SEM) using a JEOL 7800 microscope operated at 1.5 kV (gentle beam mode). EDS mapping was carried out from JEOL 2100 operated at 200 kV. Electron tomography (ET) was obtained by a Tecnai G2 F30 (FEI) operated at 300 kV. The ET specimens were prepared by depositing nanoparticle/ethanol suspension onto a formvar film

supported copper grid (hexagon 50 mesh, Electron Microscopy Science). Micromeritics Tristar 3020 was used to carry out nitrogen sorption analysis. The specific surface areas and pore size distributions of IONP@D-SiO_2 were calculated by using the Brunauer-Emmett-Teller (BET) method and Barret-Joyner-Halenda (BJH) method derived from the adsorption branch of the isotherms, respectively. The particle size distribution and zeta potential of IONP@D-SiO_2 in both Phosphate-buffered saline (PBS) and DMEM (+10% FBS) were determined by using a Zetasizer Nano-ZS from Malvern Instrument at 25 °C.

Iron release profile of IONP@D-SiO_2 in PBS (pH 5)

100 μg/mL of IONP@D-SiO_2 was incubated in 1 mL of PBS (pH5) and placed in a shaker at 37°C. At selected time point, the suspension was centrifuged at 15000 rpm for 10 min. 950 μL of supernatant was collected and replaced by 950 μL of fresh PBS (pH 5). The supernatant was added with 200 μL of 70% HNO_3 for Fe measurement by inductively coupled plasma-optical emission spectrometry (ICP-OES). The experiment was performed in triplicate.

Cell culture

PBS, Dulbecco's Modified Eagle Medium (DMEM) and trypsin-EDTA (0.25%) were purchased from GIBCO. Penicillin-Streptomycin (PS) was purchased from ThermoFisher Scientific. Fetal bovine serum (FBS) was purchased from Sigma-Aldrich. B16F10 melanoma cancer cells and RAW264.7 macrophages were purchased from ATCC (American Type Culture Collection) and CBA (CellBank Australia), respectively. Both raw264.7 and B16F10 cells were cultured in DMEM supplemented with 10% FBS and 1% PS at 37 °C with 5% CO_2.

To generate bone-marrow derived macrophage (BMDM), bone marrow was harvested from mice femurs and tibias according to literature.[3] 5 x 10^6 of isolated bone-marrow monocytes

were seeded in one Sterilin™ 100mm Square Petri Dish (ThermoFisher Scientific) and cultured in Roswell Park Memorial Institute (RPMI) 1640 Medium (ThermoFisher Scientific) supplemented with 10% FBS, 1% PS and 20 ng/mL of macrophage colony-stimulating factor (M-CSF, PEPROTECH) at 37 °C with 5% CO_2. On day 5, culture medium was replaced with fresh medium containing M-CSF. On day 7, cells were washed and cultured in fresh medium which contains different formulation for treatment.

Intracellular iron accumulation detection

RAW264.7 cells were seeded in 6-well microplate at a density of 3×10^5 per well. After 24 h incubation, cells were treated with 15 μg/mL of IONP@D-SiO_2, 6 μg/mL of D-SiO_2 (40% w/w of IONP@D-SiO_2), 0.04 mM of $FeSO_4$ or 0.04 mM of $FeCl_3$. The molarity of Fe in $FeSO_4$ and $FeCl_3$ was equal to the molarity of Fe^{2+} in Fe_3O_4@D-SiO_2. At selected time point, cells were detached from plate, washed and suspended in 1 mL of PBS, followed by cell counting. Then the cells were centrifuged at 300 g for 5 min and transferred to 200 μL of diH_2O for cell lysis with the aid of ultra-sonication for 1 h. After centrifugation at 15000 rpm for 10 min, the pellet was removed. The supernatant containing free ions and various proteins. 15% HNO_3 was used to extract iron from iron-binding proteins in the supernatant. Finally, the soluble iron in solution was measured by ICP-OES. Normalization of intracellular iron accumulation was calculated by the following equation at each time point. $R = \frac{intracellular\ iron\ amount\ of\ treated\ groups}{intracellular\ iron\ amount\ of\ untreated\ groups}$. The experiments were performed in triplicate.

Intracellular ROS measurement

RAW264.7 cells were seeded in 6-well microplate at a density of 3×10^5 per well and incubated at 37°C for 24 h. Then, the cells were washed twice with PBS followed by incubation with fresh media containing IONP@D-SiO_2 (15 μg/mL), D-SiO_2 (6 μg/mL), $FeSO_4$ (0.04 mM) or $FeCl_3$ (0.04 mM) at selected time point. After a certain period, media was removed and 20 μM of 2', 7'-dichlorofluorescein diacetate (DCFDA) in PBS was added to cells for 20 min incubation at 37°C. Afterwards, DFDCA solution was removed. The cells were detached by cold PBS. The intensity of fluorescence with excitation peak of 488 nm was measured by flow cytometry (FACS). The experiments were performed in triplicate.

Cell viability test

10,000 cells/well of RAW264.7 cells or 5,000 cells/well B16F10 cells were seeded in 96-well plates, respectively. The next day, cells were treated with PBS, IONP@D-SiO_2 and D-SiO_2 at various concentrations. After 24 h incubation, cell viability was determined by using 3-(4, 5-Dimethylthiazol-2- yl)-2, 5- diphenyl tetrazolium bromide) assay (MTT). The experiments were performed in triplicate.

Cellular uptake

RAW264.7 cells were seeded in 6-well microplate at a density of 3×10^5 per well and incubated at 37°C for 24 h. Then, cells were incubated with IONP@D-SiO_2 (15 μg/mL) and D-SiO_2 (6 μg/mL) for 12 h. After washing, collection and counting, cells were then lysed by diH_2O with the aid of ultra-sonication, followed by centrifugation at 15000 rpm for 10 min. The supernatants were removed. 1 M of NaOH aqueous solution was added to allow dissolution of Si content. The Si concentration was determined by ICP-OES. The experiments were performed in triplicate.

Determination of macrophage polarization and signaling pathway analysis

Expression of CD80, CD86, CD64 induced by IONP@D-SiO_2 and D-SiO_2 was determined by flow cytometry. Gene expression of CD206, Arg-1, iNOS, IL-23, CXCL10, CCL2, TNF-α and four transcription factors (STAT1, NF-κB, AP-1 and IRF5) was evaluated by quantitative RT-PCR (qPCR). The protein expression level of four transcription factors and ferritin was investigated by western blot in both RAW264.7 cells and BMDM. For M2 macrophages, RAW264.7 cells were treated with IL-4 (20 ng/mL) for 24 h according to literature. [4-5] For flow cytometry analysis, RAW264.7 cells were treated with IONP@D-SiO_2 (15 μg/mL), D-SiO_2 (6 μg/mL), lipopolysaccharide (LPS) (100 ng/mL, Sigma-Aldrich) or interleukin 4 (IL-4) (20 ng/mL, Abcam) for 24 h. Then the cells were harvested, washed and incubated with Fc Block (TruStain fcX™ (anti-mouse CD16/32) Antibody, BioLegend) for 10 min, followed by surface staining with anti-CD80, anti-CD86 and anti-CD64 antibody (BioLegend) for 30 min before analyzed by flow cytometry. For qPCR analysis, after 12 h treatment of IONP@D-SiO_2 (15 μg/mL), D-SiO_2 (6 μg/mL) or LPS (100 ng/mL), raw 264.7 cells (M*0* or M2) were harvested followed by RNA extraction with the RNeasy mini kit (Qiagen, Valencia, CA, USA). 1 μg of total RNA was reverse-transcribed into complementary DNA with High Capacity cDNA Reverse Transcription Kits (ThermoFisher Scientific). qPCR was performed by using a SYBR® Green PCR Master Mix (Invitrogen) kit with primers described below. Cycling conditions were according to manufacturer's protocol. All experiments were performed in triplicate.

Primer	Forward (5'-3')	Reverse (5'-3')
Gusb	CAGTTGTGTGGGTGAATGGGA	CACTCTGGACCAGCTTGCTA
Arg-1	TACAAGACAGGGCTCCTTTCAG	CGTTGAGTTCCGAAGCAAGC

CD206	GCTGGCGAGCATCAAGAGTA	AGGAAACGGGAGAACCATCAC
iNOS	TGCTTTGTGCGAAGTGTCAG	CCCTTTGTGCTGGGAGTCAT
IL23a p19	CTGCTCTGTCCCTCAGTTCTAA	TTGTCAGTTCGTATTGGTAGTCC
STAT1	GTCATCCCGCAGAGAGAACG	GCAGAGCTGAAACGACCTAGA
NF- κB	CCTGCTTCTGGAGGGTGATG	GCCGCTATATGCAGAGGTGT
AP-1	TTGTTACAGAAGCGGGGACG	GAGGGCATCGTCGTAGAAGG
IRF5	CCCTGTCCCAGACCCAAATC	AGGTCCGTCAAAGGCAACAT
CXCL10	ACGTGTTGAGATCATTGCCAC	GTCGCACCTCCACATAGCTT
CCL2	CACTCACCTGCTGCTACTCA	GCTTGGTGACAAAAACTACAGC
TNF-α	GCCTATGTCTCAGCCTCTTCTC	GCCATTTGGGAACTTCTCATCC

For Western blot, RAW264.7 cells or BMDM were treated with IONP@D-SiO_2 (15 μg/mL), D-SiO_2 (6 μg/mL), LPS (100 ng/mL, Sigma-Aldrich), IL-4 (20 ng/mL, Abcam) or interferon gamma (IFN-γ) (50 ng/mL, Abcam) for 12h. Then, cells were harvested and lysed in RIPA (Radio-Immunoprecipitation Assay) Buffer (Sigma-Aldrich) containing Protease Inhibitor Cocktail (Sigma-Aldrich). Bicinchoninic acid (BCA) assay was used to determine the concentration of protein in cell lysate. 30 μg of cell lysate protein was used for sample preparation and gel electrophoresis (Bio-Rad). The primary antibodies used were anti-STAT1-α, anti-STAT1-phospho, anti-NF-κB, anti-C-JUN, anti-IRF5, anti-ferritin purchased from Abcam and anti-actin purchased from Cell Signaling Technology. IRDye 800CW Goat anti-Rabbit IgG and IRDye 680LT Goat anti-Mouse IgG (LI-COR Biosciences) were used as secondary antibodies. The blots were detected by using Odyssey ® CLx Infrared Imaging System (LI-COR Biosciences). The experiments were repeated twice.

Immunofluorescence microscopy (ubiquitination of TRAF6)

IONP@D-SiO_2 and D-SiO_2 were grated with Rhodamine B isothiocyanate (RITC, Sigma-Aldrich) firstly. Briefly, 3 mg of RITC was reacted with 20 μL of (3-aminopropyl) triethoxysilane (APTES) in 1 mL of ethanol under vigorously stirring in dark for 24 h. Afterwards, 2 mg of nanoparticles were immersed in 1 mL of RITC-APTES solution in dark for 24h. The RITC-labelled nanoparticles were collected and washed by ethanol several times to remove free dye molecules.

RAW264.7 cells were seeded on a sterile coverslip in a 12-well plate at a density of 1.5×10^5 cells per well. Then, the cells were treated with IONP@D-SiO_2 (15 μg/mL), D-SiO_2 (6 μg/mL) or LPS (100 ng/mL) at 37°C for 0.5 h. The cells were washed with PBS twice and fixed with 4% paraformaldehyde (PFA) for 30 min. After three washes with PBS, cells were permeabilized with 0.1% Triton X-100 in cold PBS for 15 min. Then, the cells were blocked by 5% non-fat milk for 1 h at room temperature with gentle shaking. The intracellular staining was performed by incubation of primary antibody against TRAF6 (ThermoFisher) and ubiquitin (ThermoFisher) in 5% non-fat milk at 4°C overnight. The cells were washed with PBS three times for 5 min per time. The cells were further incubated with corresponding secondary antibodies (Alexa Fluor® 488 goat Anti-Rabbit IgG H&L and Alexa Fluor® 647 goat Anti-Mouse IgG H&L, Abcam) for 2 h at room temperature. After washing cells again, the nuclei were stained with DAPI. Finally, the coverslips were taken out, sticked on glass slides and observed at ×63 magnification under confocal laser scanning microscopy (Leica SP8) using 405 nm, 488 nm, 555 nm and 647 nm for viewing nuclei, TRAF6, nanoparticles and ubiquitin, respectively. The experiments were performed in triplicate.

***In vivo* anti-tumor studies**

All *in vivo* experiments were approved by the Animal Ethic Unit in The University of Queensland. Female C57BL/6 mice (6-8 weeks of age) were purchased from Biological Resource Facilities, the University of Queensland. For prophylactic tumor model, C57BL/6 mice were implanted with 1×10^5 of B16F10 cells into the right flank with or without 300 μg of IONP@D-SiO_2 (15 mg/kg) on day 1. Tumor growth and mouse weight were monitored for up to 21 days (n=6 mice) after implantation. Survival rate was monitored for up to 50 days (n=7) after implantation. From day 8, tumor in PBS group were measurable, so tumor volume was started to record. The mice were euthanized on day 21 (two mice in PBS group were euthanized on day 19 when total volume of tumors were more than 1000 mm^3). The spleens were collected to analyze population of cytotoxic T lymphocytes (CTL). The *in vivo* anti-tumor study was repeated twice.

***In vivo* M1 and M2 macrophage test**

Tumors were obtained on day 12 for flow cytometric analysis and immunofluorescence assay. For flow cytometry, tumors were digested by 1mg/mL of Collagenase A (Roche) and 100 U/mL of DNase I (Roche) in serum-free DMEM. Single cell suspension were prepared via passing through a cell strainer after tumor digestion. The cells were washed in PBS containing 0.1% BSA and treated with red blood cells (RBCs) lysis buffer for 5 min to lyse RBCs. The reaction was stopped by adding PBS, followed by washing and centrifugation of cells. Trypan blue and hemocytometer were used to count cells before staining. Then, cells were blocked with Fc Block (TruStain fcX™ (anti-mouse CD16/32) Antibody, BioLegend) for 10 min, followed by surface staining with anti-mouse F4/80 (PE/Cy7, BioLegend) and anti-CD80 (APC, BioLegend) at 4°C for 30 min in dark. Finally, the cells were washed and fixed with 4% PFA before analysis in flow cytometry. The experiment was performed in triplicate. For immunofluorescence assay, tumors were embedded in Tissue-Tek OCT gel and frozen on dry ice after collection. Then the samples were sectioned and processed as previously described.[6]

Anti-mouse CD206 (Abcam) and anti-mouse F4/80 (Abcam) were used. The glass slides were observed at ×20 magnification under confocal laser scanning microscopy (Leica SP8) using 405 nm, 488 nm and 530 nm for viewing nuclei, CD206 and F4/80, respectively.

In vivo CTL test

Single splenocytes were obtained on day 21 for a flow cytometric analysis. To prepare single cell suspension, cell strainers were used to process fresh spleens. The cells were washed twice with PBS containing 0.1% bovine serum albumin (BSA) and 0.6% sodium citrate. Then, 2.5 mg/L of DNase in PBS containing 0.1% BSA and 0.6% sodium citrate (with Ca^{2+} and Mg^{2+}) was used to avoid cell clumping resulting from released DNA. Then, the cells were treated with RBCs lysis buffer for 5 min to lyse RBCs. The reaction was stopped by adding PBS, followed by washing and centrifugation of cells. After removal of supernatant, the cells were suspended in PBS (+0.1% BSA). Trypan blue was applied for cells to discriminate dead cells during cell counting. Then, the cells were incubated with Fc Block (TruStain fcX™ (anti-mouse CD16/32) Antibody, BioLegend) for 10 min, followed by surface staining with anti-mouse CD3 (Brilliant Violet 421, BioLegend), CD4 (PE, BioLegend) and CD8 (PerCPCyanine5.5, eBioscience) at 4°C for 30 min in dark. Finally, the cells were washed and fixed with 4% PFA before analysis in flow cytometry. The experiment was performed in four replicates.

Statistical analyses

Two-way ANOVA was used to perform statistical analyses in Scheme.1 (tumor volume), Fig.1f, Fig.2a-b, Fig.3a, Fig.S7 and Fig.S11c. One-way ANOVA was used in the rest of data. Stars represented p value as following: * $p < 0.05$, ** $p < 0.01$, *** $p < 0.001$, **** $p < 0.0001$. n.s. means no significant difference.

Table S1. Surface charge and dispersity of IONP@D-SiO_2 in PBS and DMEM (+10% FBS) solution. Surface area and pore volume of IONP@D-SiO_2.

	Surface charge (eV)		PDI			
	PBS	DMEM	PBS	DMEM	Surface area (m^2/g)	Pore volume (cm^3/g)
Fe_3O_4@D-SiO_2	-16.10 ± 0.90	-4.43 ± 1.49	0.208 ± 0.016	0.273 ± 0.027	191.9	0.61
Fe_2O_3@D-SiO_2	-14.63 ± 1.37	-6.31 ± 0.77	0.160 ± 0.036	0.200 ± 0.019	188.6	0.55

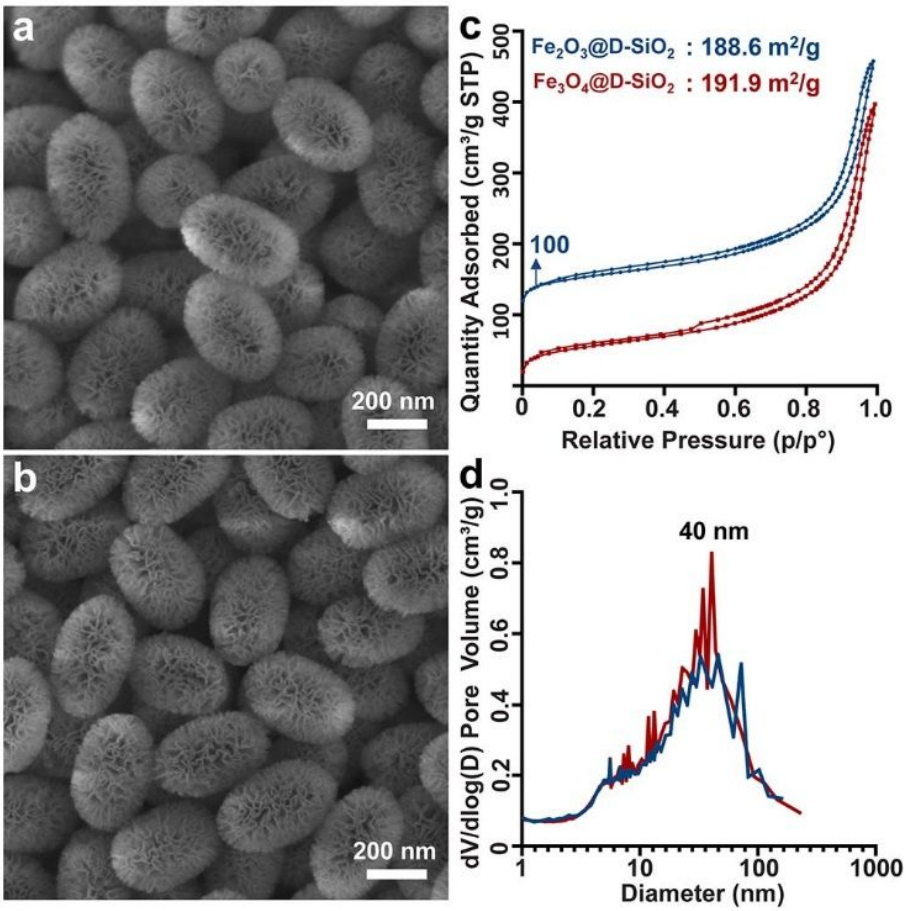

Figure S1. SEM images of (a) Fe_2O_3@D-SiO_2 and (b) Fe_3O_4@D-SiO_2 nanoparticles. N_2 sorption isotherm plots (c) and corresponding BJH pore size distribution curves (d) calculated from adsorption branches of IONP@D-SiO_2.

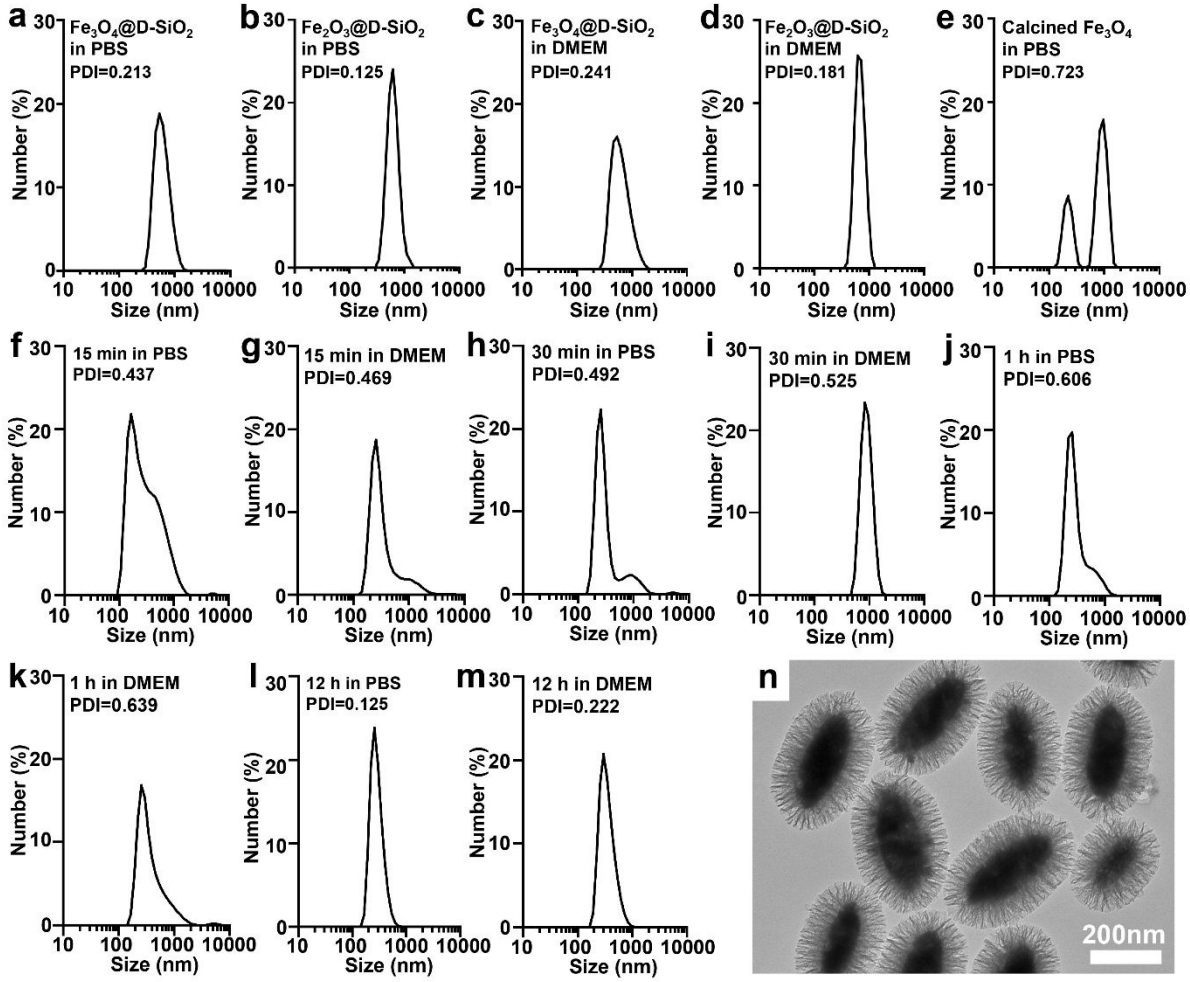

Figure S2. Particle size distribution curves of Fe_3O_4@D-SiO_2 (a, c), Fe_2O_3@D-SiO_2 (b, d) and calcined Fe_3O_4 nanoparticles measured at the same concentration in PBS or DMEM (+10% FBS) by dynamic light scattering (DLS) immediately after preparation of particle suspension. Long term stability of Fe_3O_4@D-SiO_2 dispersion was investigated by measuring the particle size distribution curves at 15 min (f, g), 30 min (g, i), 1h (j,k) and 12h (l, m) after preparation of particle suspension. (n) TEM image of Fe_3O_4@D-SiO_2 after storing in PBS solution for 1 week at 4 °C.

Figure S2 a-e show that silica shell stabilized Fe_3O_4 in both PBS solution and DMEM (+10% FBS) solution. To further confirm the stability of Fe_3O_4@D-SiO_2 suspension, particle size distribution in both PBS and DMEM (+10% FBS) was determined at different time points after preparation of particle suspension. The PDI value of particle suspension increased gradually in

1h after preparation and a small peak with large-particle size occurred at the right side of major peak (Figure S2f-k), which implies increased aggregation. After 12 h, the PDI value decreased dramatically and the peaks became sharp again (Figure S2l-m), because the aggregated nanoparticles settled down. The sedimentation of Fe_3O_4@D-SiO_2 was due to the solid nature, large particle size and high density of nanoparticles[7]. To confirm that silica shell could keep good integrity of Fe_3O_4@D-SiO_2 after long term storage, TEM images of Fe_3O_4@D-SiO_2 was taken after 1 week storage in PBS solution at 4 °C. Figure S2n demonstrated that Fe_3O_4@D-SiO_2 kept complete morphology and mono-dispersed after long-term storage.

It should be noted that in our study, subcutaneous inject was used. In order to avoid the influence of sedimentation, nanoparticle suspension was prepared and used freshly just before each *in vitro* and *in vivo* experiment. For future bio-applications of IONP@D-SiO_2 where intravenous injection is needed, PEG modification will be used to improve the colloidal stability of nanoparticles.

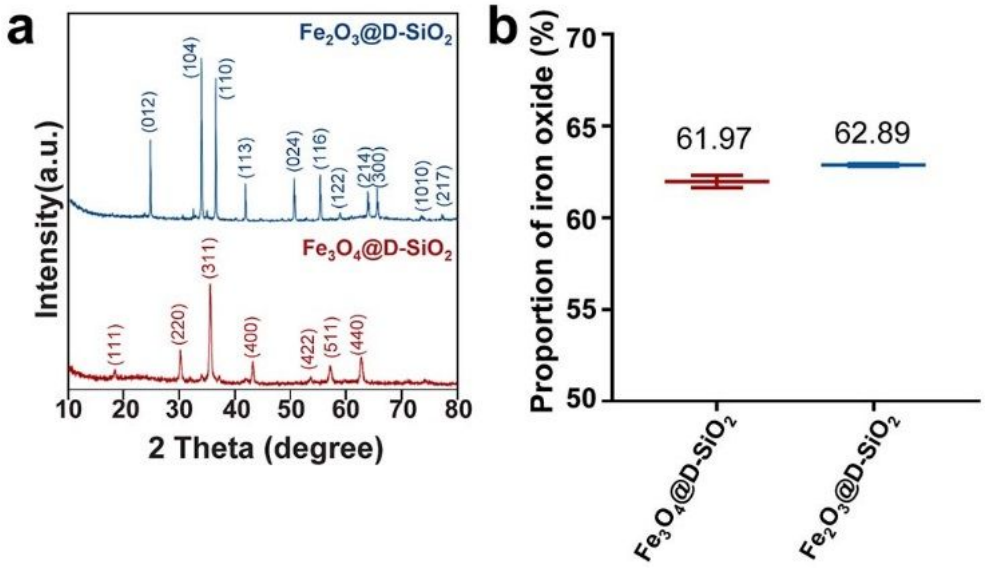

Figure S3. (a) XRD spectra of IONP@D-SiO_2. The upper and lower peaks were indexed to the crystal structures of Fe_2O_3 (JCPDS-33-0064) and Fe_3O_4 (JCPDS-65-3107) respectively, confirming the pure phase of both IONP cores. (b) Weight proportion of iron oxide core in two IONP@D-SiO_2 calculated from the Fe and Si content in nanoparticles measurement by ICP-OES. To perform ICP-OES test, IONP@D-SiO_2 nanoparticles were dissociated by 2M NaOH aqueous solution and 2M HCl aqueous solution, respectively. The weight ratio of Fe to Si was around 2.525 in Fe_3O_4@D-SiO_2 and 2.538 in Fe_2O_3@D-SiO_2.

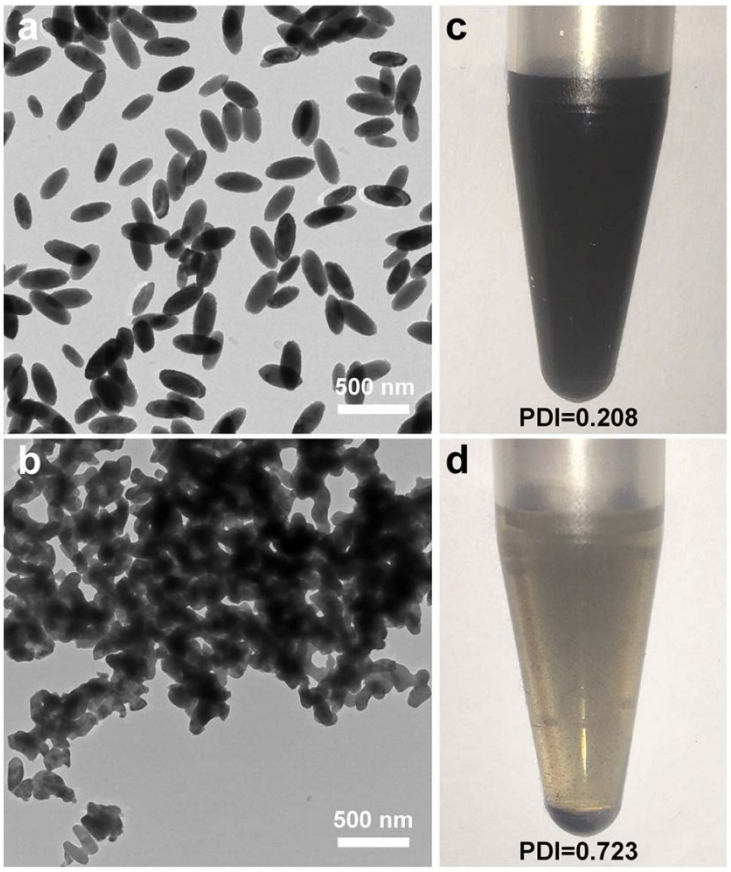

Figure S4. TEM images of (a) as-prepared Fe_2O_3 nanoparticles and (b) corresponding Fe_3O_4 nanoparticles after thermal treatment. Photos of (c) Fe_3O_4@D-SiO_2 and (d) calcined Fe_3O_4 nanoparticles at the same concentration in PBS solution with the aid of 5 second of ultra-sonication. The PDI value was determined by dynamic light scattering (DLS).

As-prepared Fe_2O_3 nanoparticles were well dispersed in PBS solution. Without confinement of silica shell, Fe_3O_4 nanoparticles showed heavy aggregates and changed shape due to magnetic interaction and recrystallization during thermal treatment. With silica shell, Fe_3O_4@D-SiO_2 were well dispersed in PBS, showing uniform black color. In contrast, Fe_3O_4/PBS suspension showed obvious black precipitates at the bottom of tube and light grey in upper suspension. The PDI value of Fe_3O_4@D-SiO_2 and Fe_3O_4 supported the difference in sedimentation behavior of two nanoparticles as well. Results in Figure S4 demonstrated the significance of silica shell in maintaining shape and dispersity of IONP during thermal conversion.

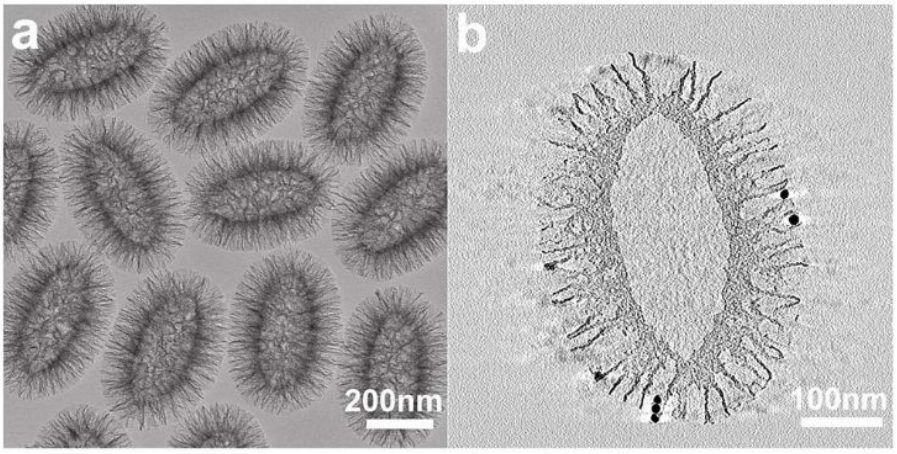

Figure S5. TEM image and electron tomogram (ET) slice of hollow D-SiO_2 synthesized by removing Fe_3O_4 core in 2M HCl/ethanol solution. Black dots are colloidal gold particles (10 nm) deposited on D-SiO_2 as fiducial markers for the image alignment procedures.

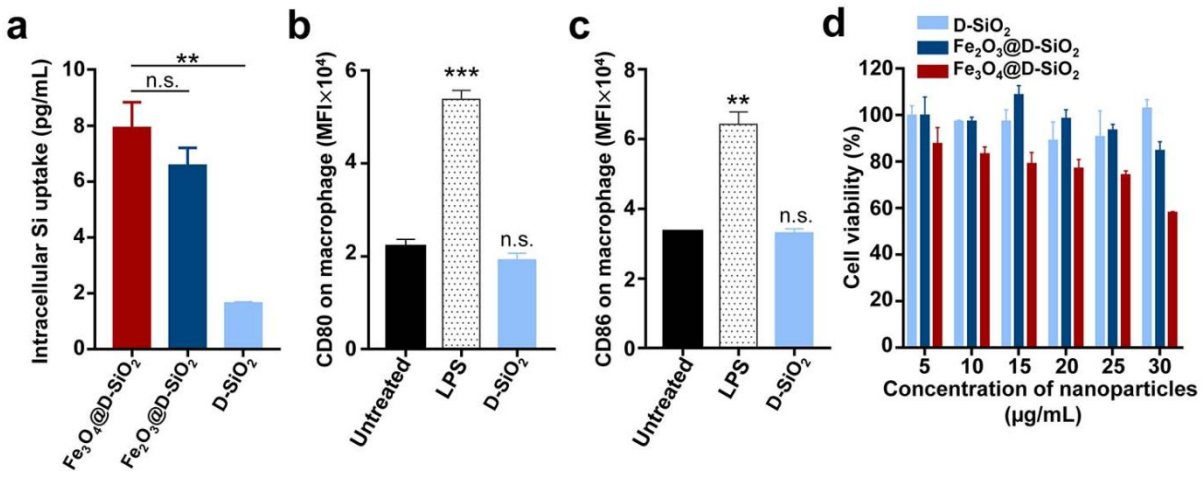

Figure S6. (a) Cellular uptake of IONP@D-SiO_2 and D-SiO_2 nanoparticles at 12 h time point, verified by measuring Si content in cells via ICP test. Flow cytometry analysis of CD80 (b) and CD86 (c) surface marker expression on macrophage after 24h treatment with 25 μg/mL of D-SiO_2. (d) Cell viability of macrophage treated with IONP@D-SiO_2 and D-SiO_2 in varying concentrations. * in (b-c) indicates the difference of treated group compared to untreated group.

The toxicity profile of IONP@D-SiO_2 was shown in Figure S6d, representing that Fe_3O_4@D-SiO_2 was more toxic than Fe_2O_3@D-SiO_2 due to higher ROS generation from magnetite core. Based on this profile, 15 μg/mL was chosen as the concentration of IONP@D-SiO_2 in all *in vitro* studies. 6 μg/mL of D-SiO_2 was used according to the proportion of SiO_2 content in IONP@D-SiO_2. Figure S6a illustrated the uptake of three nanoparticles in macrophage after 12 h treatment. Fe_3O_4@D-SiO_2 had slightly higher uptake than Fe_2O_3@D-SiO_2. This was resulted from magnetic attraction-induced aggregates, as demonstrated in Table S1 (PDI of Fe_3O_4@D-SiO_2 in DMEM was 0.273, slightly large than 0.200 of Fe_2O_3@D-SiO_2). The uptake of D-SiO_2 was not comparable to IONP@D-SiO_2, exhibiting 4 fold lower intracellular Si amount. This may be attributed to the significant lower density and hollow structure of D-SiO_2. The solid nature and higher density of nanoparticles improved sedimentation and hence increased effective dosage of nanoparticle exposed to cells, which has been demonstrated by Mostafa Yazdimamaghani and coworkers[7]. To eliminate the influence of D-SiO_2 on

macrophage activation, high dosage of D-SiO_2 (25 μg/mL, 4 fold of 6 μg/mL) was used to treat M*0* macrophage and corresponding M1 marker expression was further determined (Figure S6b-c). The results showed that D-SiO_2 cannot polarize M*0* to M1. The influence of D-SiO_2 was negligible.

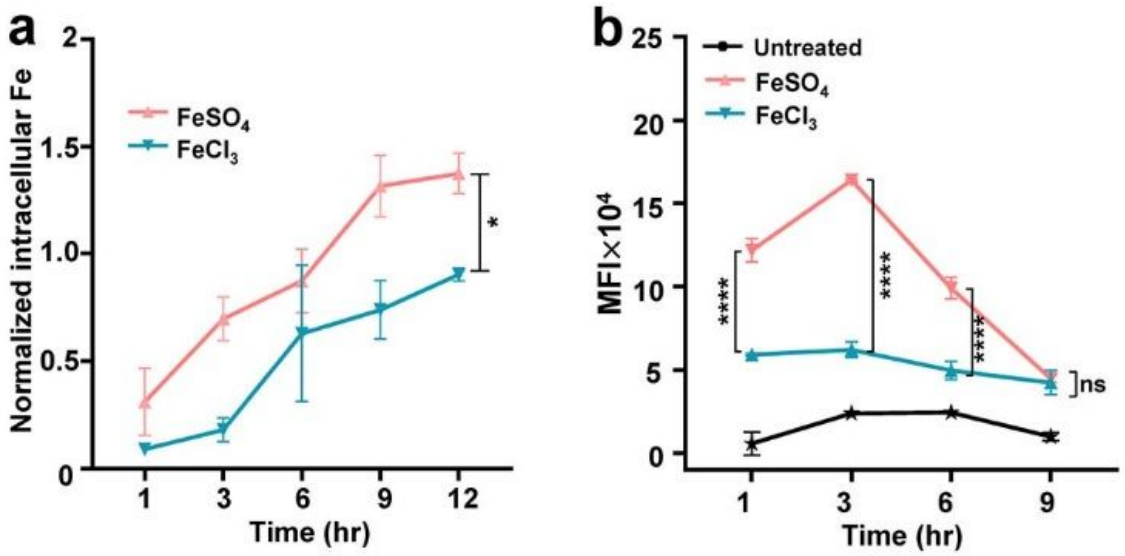

Figure S7. (a) Time-dependent intracellular iron accumulation normalized to the untreated group and (b) intracellular ROS generation. Compared to $FeCl_3$, $FeSO_4$ group showed a significant higher level of ROS generation even its corresponding intracellular iron level was lower than untreated group, implying the excellent Fenton catalyst performance of Fe^{2+}.[8]

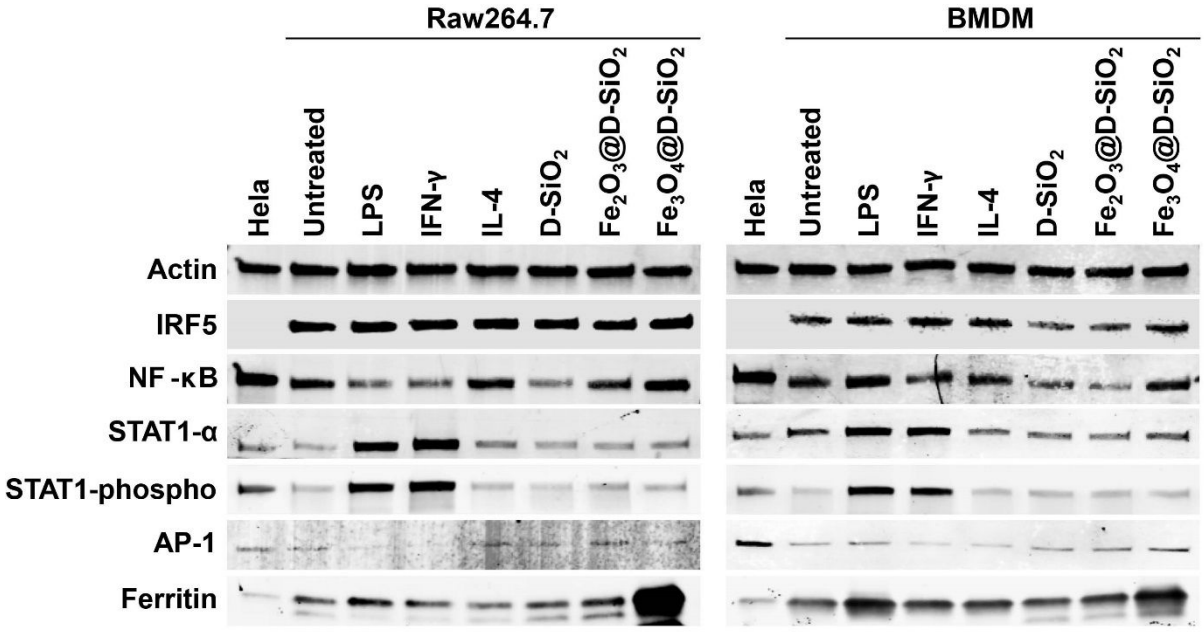

Figure S8. Signaling pathway study of M*0* macrophage (RAW264.7 and BMDM) after 12 h treatment with LPS, IFN-γ, IL-4, IONP@D-SiO_2 and D-SiO_2. The protein expression levels were measured by western blot. Hela lysate is positive control for expression NF-κB, AP-1, STAT1-α and STAT1-phospho to guarantee the correct performance of corresponding antibodies according to manuals from manufacture.

To further confirm the IONP-induced M1 signaling pathway, the activation of four transcription factors was verified by western blot at protein levels in both RAW264.7 and BMDM cells. In this experiment, IFN-γ was included as another positive control because it has been reported to activate STAT1[9]. Phosphorylation of STAT1 was used to confirm the activation of STAT1. Figure S8 shows that Fe_3O_4@D-SiO_2 induced high expression levels of IRF5 and NF-κB as well as low expression levels of STAT1-α (including STAT1-phospho) and AP-1 in both RAW264.7 cells and BMDM cells, which is consistent with qPCR result in Figure 3. Together, the distinct transcription factor activation pathway of magnetite from that of molecular M1 ligand, LPS and IFN-γ is demonstrated. Ferritin (an iron storage protein)[10]

expression was also determined to confirm the intracellular iron storage in both macrophage cell lines. An extremely high expression level of ferritin in Fe_3O_4@D-SiO_2 group further confirmed that magnetite induced a high level of intracellular iron in macrophage which played a significant role in M1 macrophage activation.

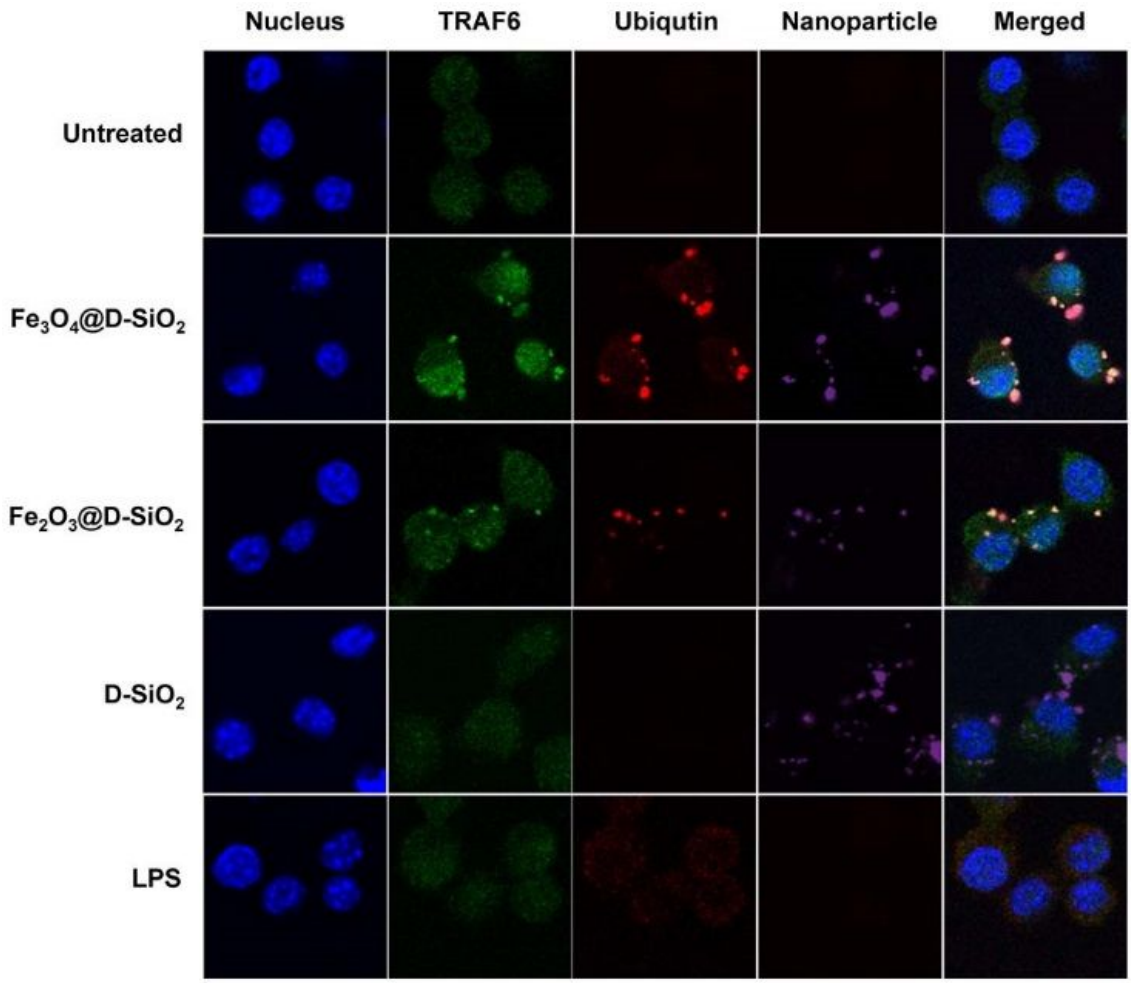

Figure S9. The activation of TRAF6 (upstream of IRF5) in IONP@D-SiO_2 treated macrophages, confirmed by the co-localization of TRAF6, ubiquitin and IONP@D-SiO_2 nanoparticles. Macrophages were treated with different formulations for 0.5h and stained for nucleus (DAPI, blue), TRAF 6 (Alexa Fluor 488, green) and ubiquitin (Alexa Fluo 647, red). The nanoparticles were stained with RITC (purple).

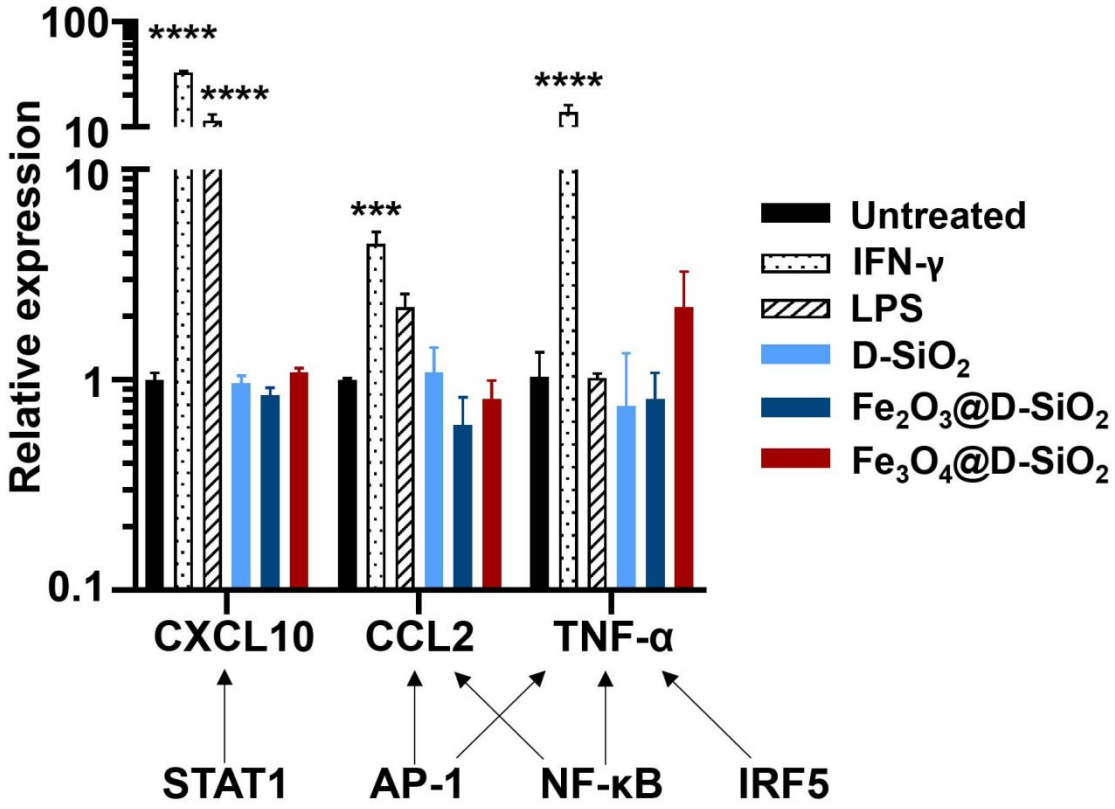

Figure S10. Gene expression levels of M1 markers (CXCL10, CCL2 and TNF-α) of M*0* macrophage (RAW264.7) treated with LPS, IFN-γ, IONP@D-SiO_2 and D-SiO_2 determined by qPCR relative to untreated group.

As the signaling pathway study (Figure 3a and Figure S9) shows that IONP activated IRF5 and NF-κB, but not STAT1 and AP-1, therefore more M1 markers were investigated by determining the gene expression levels of CXCL10 (downstream of STAT1)[11], CCL2 (downstream of AP-1 and NF-κB)[12] and TNF-α (downstream of NF-κB and IRF5).[11] Figure S10 shows that negligible expression of CXCL10 and CCL2 in Fe_3O_4@D-SiO_2 group compared to untreated group, further showing that magnetite-induced M1 polarization did not rely on the activation of STAT1 and AP-1. Because iNOS (Figure 3b), the downstream of NF-κB, showed negligible expression in Fe_3O_4@D-SiO_2 group, the slightly increased expression of TNF-α in Fe_3O_4@D-SiO_2 group may result from the activation of IRF5.

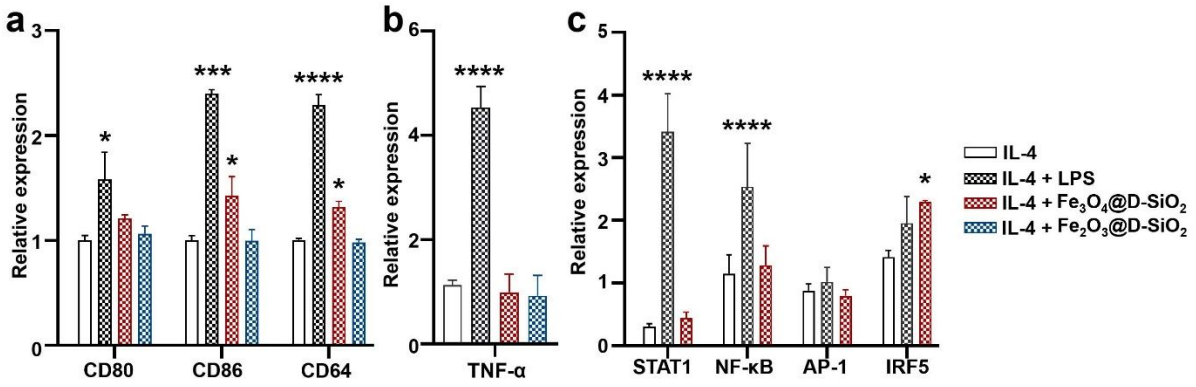

Figure S11. Re-activation study of M2 macrophage (Raw264.7) treated with LPS and IONP@D-SiO_2. CD80/CD86/CD64 expression (a) was analyzed by flow cytometry while TNF-α gene expression (b) was determined by qPCR. The activation of different signaling pathway in reprogrammed macrophages (M2) treated by Fe_3O_4@D-SiO_2 (c) was measured by qPCR. * in (c-d) indicates the difference of treated group compared to IL-4-treated group (untreated M2 group).

The up-regulated M1 markers in magnetite-treated M*0* macrophage were further investigated in IONP-treated M2 macrophage. Figure S11 shows that M1 surface markers (CD80/86/64) exhibited slight up-regulation induced by Fe_3O_4@D-SiO_2. Because Fe_3O_4@D-SiO_2 could only increase TNF-α gene expression level in M*0* macrophage in small degree (Figure S10), it is more difficult for Fe_3O_4@D-SiO_2 to boost TNF-α gene expression in M2 macrophage.

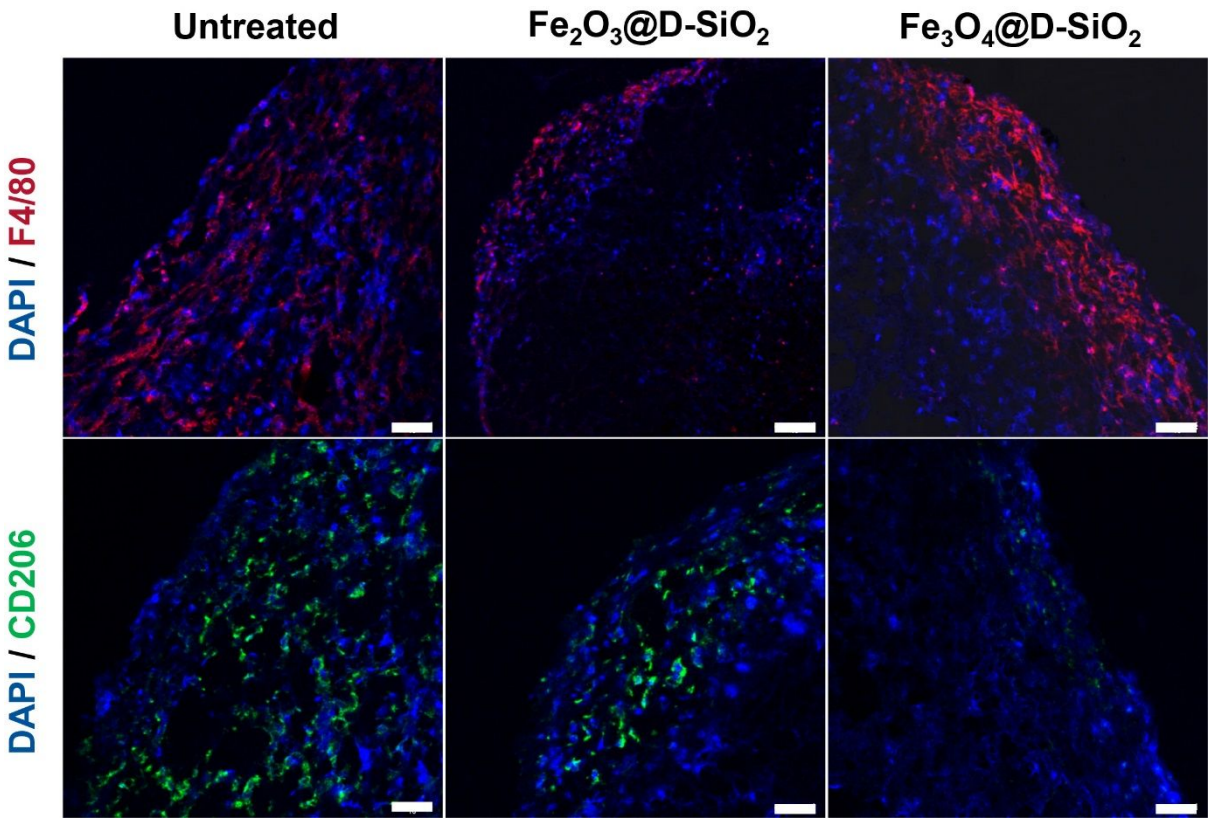

Figure S12. Representative immunofluorescence staining for F4/80 (red, R6G) and CD206 (green, FITC) of tumor sections obtained at 12 day after implantation of B16F10 cells with or without IONP@D-SiO_2. Scale bars, 10 μm.

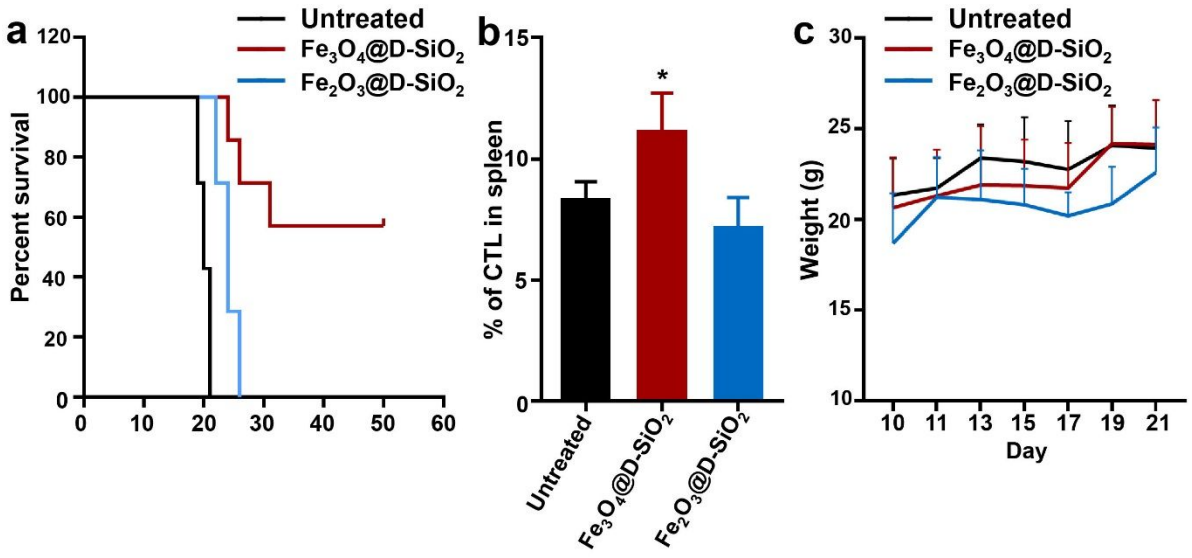

Figure S13. Survival rate (a), population of CTL in spleen (b) and weight curve (c) and of C57BL/6 mice treated with IONP@D-SiO_2 in prophylactic melanoma model. * in (a) indicates the difference of treated group compared to untreated group.

7 mice/group was used for survival investigation. Mice was sacrificed when one dimension of tumor reached 1cm according to the guidelines of Animal Ethics Committee of The University of Queensland. In Figure S13a, tumors in untreated group grew fast and all mice died within 21 days after tumor implantation. Fe_2O_3@D-SiO_2 group exhibited longer survival rate compared to untreated group with all mice died in 26 days. Fe_3O_4@D-SiO_2 group showed the longest survival rate. Tumors of 3 mice in Fe_3O_4@D-SiO_2 group decreased after 35 days and disappeared after 40 days.

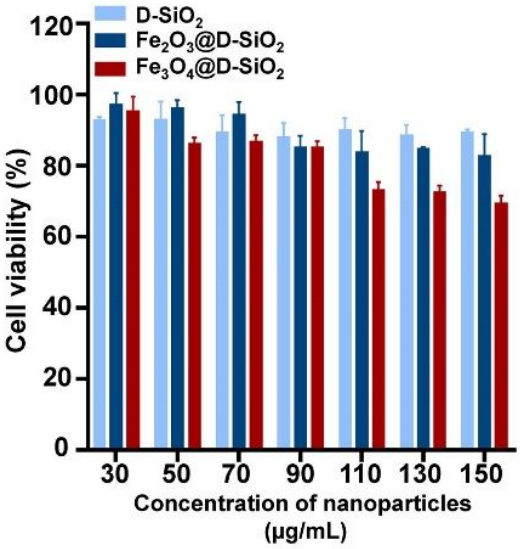

Figure S14. Cell viability of B16F10 treated with IONP@D-SiO_2 and D-SiO_2 in varying concentrations.

The original seeding density of B16F10 was 5,000 cells per well. After one day incubation, cells numbers were over 10,000 when treated with nanoparticles according to doubling time of B16F10 in literatures.[13-14] Because cell viability was performed in 96-well plate, in which 200 μL was the total volume. Hence, the highest nanoparticle weight used in this experiment was 30 μg/well. The highest ratio of nanoparticle weight to cell number in this figure is around 3×10^{-3}μg/cell, which showed acceptable 70% of cell viability.

Table S2. The Fe concentration used in *in vitro* and *in vivo* studies.

	In vitro		In vivo	
concentration	Fe_3O_4@D-SiO_2	Fe_2O_3@D-SiO_2	Fe_3O_4@D-SiO_2	Fe_2O_3@D-SiO_2
Fe	67.3 μg/mL	66.3 μg/mL	1.35 mg/mL	1.33 mg/mL
Fe (II)	22.3 μg/mL	0	0.45 mg/mL	0
Fe (III)	45.0 μg/mL	66.3 μg/mL	0.9 mg/mL	1.33 mg/mL

In *in vivo* study, we injected cancer cells together with nanoparticles subcutaneously. The ratio of particle weight to cancer cell number was 3×10^{-3}μg/cell, which was the same as the ratio used in *in vitro* study, showing an acceptable 70% cell viability (Figure S14). Hence, the dosage of IONP@D-SiO_2 used in *in vivo* study would not cause severe toxicity to cancer, suggesting that IONP-induced tumor inhibition was not mainly resulted from the toxicity of IONP@D-SiO_2. The concentration of Fe (including Fe (II) and Fe (III)) used in *in vivo* study was shown in Table S2, calculated by ICP result of Fe content measurement.

References

1. Sugimoto, T.; Wang, Y. S.; Itoh, H.; Muramatsu, A., Systematic control of size, shape and internal structure of monodisperse alpha-Fe_2O_3 particles. *Colloids Surf A* 1998, 134 (3), 265-279.
2. Yang, Y. N.; Bernardi, S.; Song, H.; Zhang, J.; Yu, M. H.; Reid, J. C.; Strounina, E.; Searles, D. J.; Yu, C. Z., Anion assisted synthesis of large pore hollow dendritic mesoporous organosilica nanoparticles: understanding the composition gradient. *Chem Mater* 2016, 28 (3), 704-707.
3. 1. Trouplin, V.; Boucherit, N.; Gorvel, L.; Conti, F.; Mottola, G.; Ghigo, E., Bone Marrow-derived Macrophage Production. *J Vis Exp* 2013, (81), e50966-e50966.
4. Vogel, D. Y. S.; Glim, J. E.; Stavenuiter, A. W. D.; Breur, M.; Heijnen, P.; Amor, S.; Dijkstra, C. D.; Beelen, R. H. J., Human macrophage polarization in vitro: maturation and activation methods compared. *Immunobiology* 2014, 219 (9), 695-703.
5. Herd, H. L.; Bartlett, K. T.; Gustafson, J. A.; McGill, L. D.; Ghandehari, H., Macrophage silica nanoparticle response is phenotypically dependent. *Biomaterials* 2015, 53, 574-582.
6. Zanganeh, S.; Hutter, G.; Spitler, R.; Lenkov, O.; Mahmoudi, M.; Shaw, A.; Pajarinen, J. S.; Nejadnik, H.; Goodman, S.; Moseley, M.; Coussens, L. M.; Daldrup-Link, H. E., *Nat Nanotechnol* 2016, 11 (11), 986-994.
7. Yazdimamaghani, M.; Barber, Z. B.; Moghaddam, S. P. H.; Ghandehari, H., Influence of silica nanoparticle density and flow conditions on sedimentation, cell uptake, and cytotoxicity. *Mol Pharmaceut* 2018, 15 (6), 2372-2383.
8. Barbusinski, K., Fenton reaction - controversy concerning the chemistry. *Ecol Chem Eng S* 2009, 16 (3), 347-358.
9. Lawrence, T.; Natoli, G., Transcriptional regulation of macrophage polarization: enabling diversity with identity. *Nat Rev Immunol* 2011, 11, 750-761.
10. Soares, M. P.; Hamza, I., Macrophages and Iron Metabolism. *Immunity* 2016, 44 (3), 492-504.
11. van Dalen, F. J.; van Stevendaal, M. H. M. E.; Fennemann, F. L.; Verdoes, M.; Ilina, O., Molecular Repolarisation of Tumour-Associated Macrophages. *Molecules* 2019, 24 (1), 9-34.
12. Akhter, N.; Hasan, A.; Shenouda, S.; Wilson, A.; Kochumon, S.; Ali, S.; Tuomilehto, J.; Sindhu, S.; Ahmad, R., TLR4/MyD88 -mediated CCL2 production by lipopolysaccharide (endotoxin): Implications for metabolic inflammation. *J Diabetes Metab Disord* 2018, 17 (1), 77-84.
13. Danciu, C.; Falamas, A.; Dehelean, C.; Soica, C.; Radeke, H.; Barbu-Tudoran, L.; Bojin, F.; Pînzaru, S. C.; Munteanu, M. F., A characterization of four B16 murine melanoma cell sublines molecular fingerprint and proliferation behavior. *Cancer Cell Int* 2013, 13, 75-75.
14. Christophe, Y. C.; Franck, M. A.; Lluis M., M., Comparison of doubling times of B16-F10 adherent and tumorspheres-forming cells both cultured under adherent conditions. *PLoS One* 2014, 9 (2), e89644.